FLAME AND EDDY STRUCTURES IN HYDROGEN–AIR TURBULENT JET PREMIXED FLAME

M. Shimura, K. Yamawaki, Y.-S. Shim, M. Tanahashi and T. Miyauchi
Department of Mechanical and Aerospace Engineering
Tokyo Institute of Technology
2-12-1 Ookayama, Meguro-ku, Tokyo 152-8550, Japan
mshimura@navier.mes.titech.ac.jp, kyamawak@navier.mes.titech.ac.jp,
yshim@navier.mes.titech.ac.jp, mtanahas@mes.titech.ac.jp,
tmiyauch@mes.titech.ac.jp

ABSTRACT

Three-dimensional direct numerical simulation (DNS) of hydrogen–air turbulent plane jet premixed flames, which are composed of high-speed unburnt mixture gas and surrounding burnt gas for flame holding, have been conducted. Fully-developed homogeneous isotropic turbulence is superimposed on the high speed mean flow under the assumption that a turbulence gird is installed in the upstream. A detailed kinetic mechanism including 12 species and 27 elementary reactions is considered. Eddy structures which have large-scale in space and streamwise rotating axis are produced along the outer edge of OH layer in burnt gas. These streamwise eddies are induced by velocity difference due to strong expansion of the burnt gas. Although combustion condition of the present DNS is classified into corrugated flamelets regime, unburnt mixture islands frequently appear behind the main flame. The creation of these islands is closely related to the fine-scale eddies in the unburnt turbulence and the separated unburnt mixture is consumed rapidly by the heating from surrounding burnt gas.

INTRODUCTION

Turbulent combustion model has significant effects on accuracy of numerical prediction of combustors. Recently, a lot of approaches (Calvin, 1985; Pope, 1988; Peters, 2000; Law and Sung, 2000; Williams, 2000; Driscoll, 2008) have been attempted to develop high accuracy turbulent combustion models and these developed models are validated by using results of numerical simulations or experiments. In modeling of turbulent premixed flames, description of dynamics of flame front is one of the most important subjects in turbulent combustion research, since that is the basis of turbulent combustion models in the flamelet concept in which local burning velocity is not so far from laminar burning velocity. In the concept of flame stretch, increasing rate of flame area is expressed by flame displacement speed, flame curvature and tangential strain rate at flame front (Pope, 1988; Candel and Poinsot, 1990). In the previous studies (Poinsot et al., 1992a; Sinibaldi et al., 2003), curvature and strain rate effects have been investigated in steady or unsteady laminar flames because flame elements in turbulent flames are assumed to be laminar flame under weak stretch with small curvature. Recently, Steinberg and Driscoll (2010) have shown a model describing relationships between strain-rate and curvature stretch-rate by introducing strain-rate and wrinkling transfer function. Their model was based on results of cinema-stereoscopic particle image velocimetry only in low mean velocity Bunsen flame. To make further progress in model of turbulent premixed combustion, it is important to investigate interactions between flame structure and turbulence in shear flows.

Direct numerical simulation (DNS) with detailed kinetic mechanism is the most precise computational method (Tanahashi et al., 2000; Tanahashi et al., 2002; Nada et al., 2004). Hawkes et al. (2009) have conducted DNS of non-premixed plane jet flames and examined lower-dimensional approximations of scalar dissipation for turbulent combustion models. In our previous study (Yamawaki et al., 2010), to clarify effects of shear on turbulent flame characteristics, two-dimensional DNS of turbulent jet premixed flame has been conducted and local burning velocity has been evaluated. In obtained probability density functions (pdf) of local turbulent burning velocity, the peak locates at laminar burning velocity, whereas variance of the local burning velocity is relatively large. The results indicate a possibility of existence of flame elements which cannot be explained by the flamelet concept. On the other hand, turbulence has three-dimensional nature, and fine-scale eddies in turbulence affects flame geometry and local flame structure (Tanahashi et al., 2000; Tanahashi et al., 2002; Nada et al., 2004). Therefore, to clarify characteristics of turbulent jet premixed flame precisely, three-dimensional DNS is required. In the present study, three-dimensional DNS of hydrogen–air turbulent jet premixed flame have been conducted and characteristics of typical flame and eddy structures are discussed. Furthermore, characteristics of turbulent plane jet premixed flame are shown by comparing with those of pla-

nar turbulent premixed flame (Nada et al., 2004) both in the pdf of local heat release rate and in distributions of coherent fine-scale eddies.

NUMERICAL METHOD

The DNS code developed in our previous study (Tanahashi et al., 2000; Tanahashi et al., 2002; Nada et al., 2004) has been modified for turbulent jet premixed flame. Soret effect, Dufour effect, pressure gradient diffusion, bulk viscosity and radiative heat transfer are assumed to be negligible. The detailed kinetic mechanism which includes 12 reactive species (H_2, O_2, H_2O, O, H, OH, HO_2, H_2O_2, N_2, N, NO_2 and NO) and 27 elementary reactions is considered to represent hydrogen/air reaction in turbulence. The detailed kinetic mechanism has been picked up from Miller and Bowman (1989), Smooke and Giovangigli (1991) and Kee et al., (1986). The temperature dependence of the viscosity, the thermal conductivity and the diffusion coefficients are considered by linking CHEMKIN-II packages (Kee et al., 1989) with several modifications for vector and parallel computations.

Computational domain of DNS of turbulent plane jet premixed flame is shown in Fig. 1 with Cartesian coordinate. Turbulent plane jet premixed flame is composed of unburnt mixture flow and surrounding burnt gas flows. The governing equations are discretized by 4th-order finite difference scheme in all directions. To eliminate numerical oscillations with higher frequency than spatial resolution of the finite difference scheme, 4th-order compact finite difference filter (Lele, 1992) is applied for all directions. Time integration is conducted by 3rd-order Runge-Kutta scheme. In addition, point implicit method with VODE solver (Peter et al., 1989) is applied for the time integrations of chemical source terms in species conservation equations to reduce the computation time. Boundary conditions are Navier-Stokes characteristic boundary condition (NSCBC) (Poinsot and Lele, 1992b; Baum et al., 1994) for x and y directions and periodic for z direction.

Fully-developed homogeneous isotropic turbulence by the preliminary DNS with spectral method is superimposed on the mean flow velocity of the unburnt mixture gas under the assumption that a turbulence gird is installed in the upstream of inlet. Characteristics of the superimposed turbulence are presented in Table 1. Re_λ, Re_l, u'_{rms}, S_L, δ_F and δ_L denote Reynolds number based on Taylor micro-scale (λ), Reynolds number based on integral length scale (l), turbulent intensity, laminar burning velocity, nominal flame thickness defined by $\delta_F = \nu/S_L$ (ν: viscosity of unburnt mixture) and

Table 1. Characteristics of the superimposed homogeneous isotropic turbulence.

	Re_λ	Re_l	$u'_{\rm rms}/S_{\rm L}$	$l/\delta_{\rm F}$	$l/\delta_{\rm L}$
HJ60	60.8	199.8	1.10	180.9	3.37
HJ97	97.1	516.2	5.29	133.3	2.49
HP37	37.4	153.47	1.70	84.3	1.69
HP60	60.8	199.8	3.39	90.5	1.69

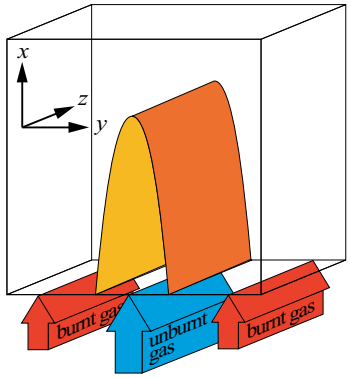

Figure 1. Computational domain.

thermal flame thickness in laminar flame, respectively. Re_λ are selected to be 60.8 and 97.1, which are called as HJ60 and HJ97 hereafter. HJ60 and HJ97 are classified into corrugated flamelets regime and boundary between corrugated flamelets regime and thin reaction zone in the turbulent combustion diagram (Peters, 2000), respectively. For comparison, the numerical conditions for turbulent premixed flame freely propagating in homogeneous isotropic turbulence is shown in Table 1 as the cases of HP37 (Tanahashi et al., 2002) and HP60 (Shim et al., 2011). Mean velocities of unburnt mixture gas are set to 100 m/s for HJ60 and 350 m/s for HJ97 to investigate effects of shear flow on flame structure. Mean velocity of burnt gases is set to 20 m/s. Equivalence ratio, temperature and pressure of unburnt mixture are selected to be 1.0, 700 K and 0.1 MPa, respectively.

Computational domains are selected to be 20 mm $\times$ 20 mm $\times$ 10 mm for HJ60 and 20 mm $\times$ 16 mm $\times$ 8 mm for HJ97. Corresponding grid points are 769 $\times$ 769 $\times$ 385 (0.228 bn.) and 1281 $\times$ 1025 $\times$ 513 (0.674 bn.), respectively. Width of nozzle for unburnt mixture is set to 5 mm. Time increment which is limited by Courant number is set to 10 ns in the present DNS.

FLAME AND EDDY STRUCTURES

Figure 2 shows a perspective drawing of instantaneous turbulent plane jet premixed flame illustrated by contour surface of temperature ($T = 1400$ K). For HJ60, overall shape of flame is Bunsen type, whereas the contour surface is distorted by turbulence motion of unburnt mixture. At the top of the flame HJ60, unburnt mixture islands are generated. These flame structures are characteristic in turbulent jet premixed flame, since unburnt mixture islands have not been found in the previous DNS of statistically planar turbulent premixed flame classified into the corrugated flamelets regime (Nada et al., 2004). As for HJ97, main flame body is enlarged by increase of inlet velocity. Flame wrinkling becomes fine due to increase of turbulent intensity and two-dimensional fluctuations in large-scale emerge in the flame structure.

Instantaneous flame and eddy structures are shown in Fig. 3 by contour surfaces of temperature ($T = 1400$ K, clear yellow) and second invariant of velocity gradient tensor ($Q(\eta/u'_{rms})^2 = 0.005$, bronze color). Distribution of OH radical mole fraction on a typical $x-y$ plane is also illustrated

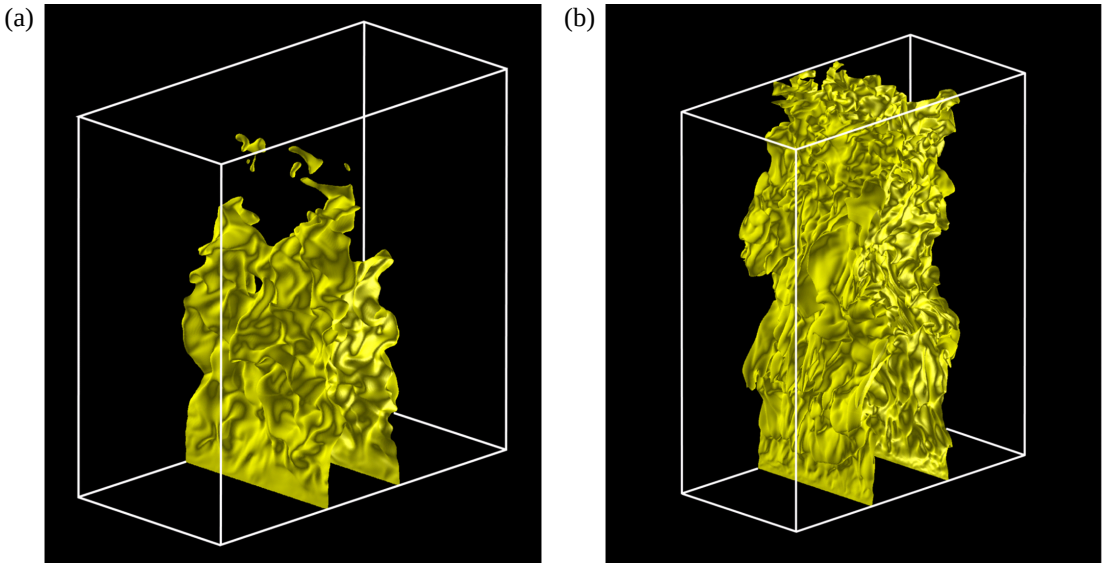

Figure 2. Instantaneous contour surfaces of temperature ($T = 1400$ K) of HJ60 (a) and HJ97 (b).

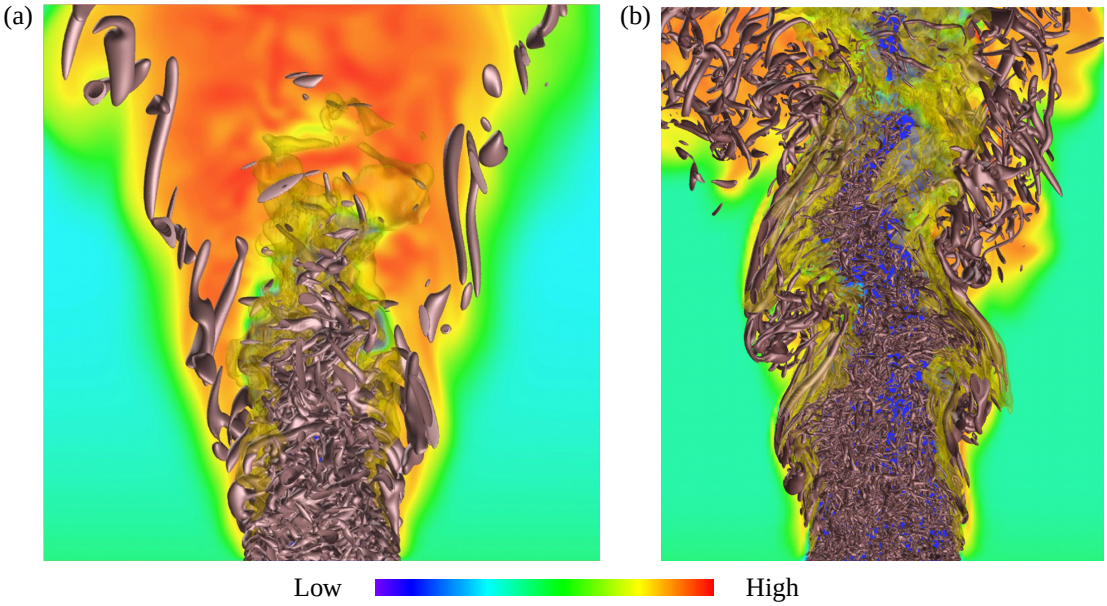

Figure 3. Instantaneous contour surfaces of temperature ($T = 1400$ K, clear yellow) and second invariant of velocity gradient tensor ($Q = 0.02 Q_{\max}$, bronze), and distribution of OH radical mole fraction on a typical $x-y$ plane for HJ60 (a) and HJ97 (b).

in Fig. 3. As for HJ60, fine-scale eddies in unburnt mixture are convected to flame front, and distort flame front significantly. Fine-scale eddies existing in the vicinity of the flame fronts decay due to the increase of viscosity and the effect of dilatation. In contrast, eddy structures which have large-scale in space and streamwise rotating axis are produced along the outer edge of high-concentration OH layer. These streamwise eddies are induced by velocity difference due to strong dilatation. For the case with high inlet velocity (HJ97), Kelvin-Helmholtz rollers are induced by the large velocity difference between unburnt and burnt gases, and the rib structures are formed in the braid region, as reported in the previous study related to turbulent mixing layer (Tanahashi et al., 2001; Wang et al., 2007). The large-scale roller and rib structures cause two-dimensionally distortion of flame structure.

The second invariant of velocity gradient tensor is used generally to understand flow field. However, the threshold for Q limits visualized eddies. Therefore, to investigate interaction between flame structures and fine-scale eddies in turbulence, axes of coherent fine-scale eddies, which are independent of threshold for visualization using Q, are identified by the method which is established in our previous study (Tanahashi et al., 1999; 2001; 2004). Figure 4(a) and (b) shows distributions of the axes of coherent fine-scale eddies and the contour surface of temperature for the case of hydrogen–air turbulent premixed flame freely-propagating in homogeneous isotropic turbulence (Nada et al., 2004) and HJ60 of the present DNS. Diameter of visualized axes of coherent

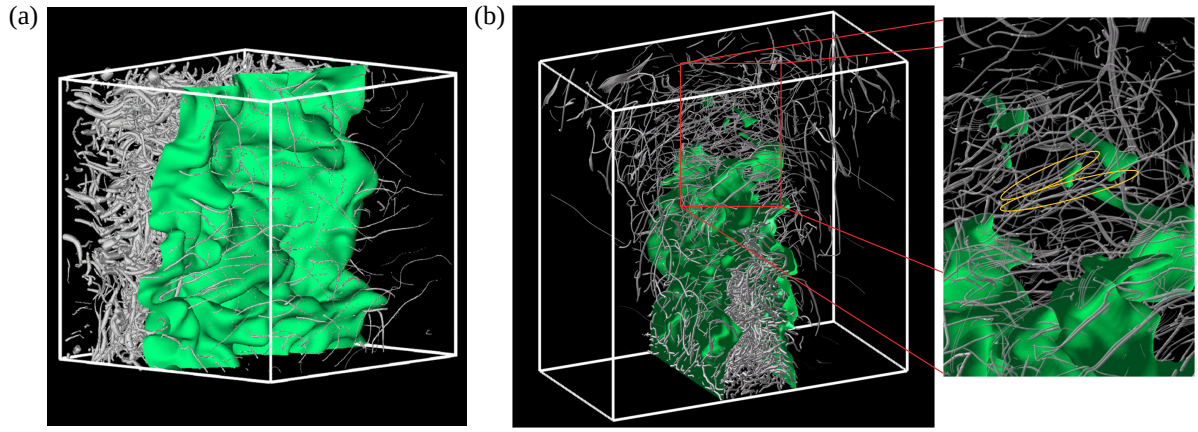

Figure 4. Examples of distributions of axes of coherent fine-scale eddies and contour surfaces of temperature ($T = 1400$ K) in planar turbulent premixed flame of HP60 (a) and turbulent jet flame of HJ60 (b).

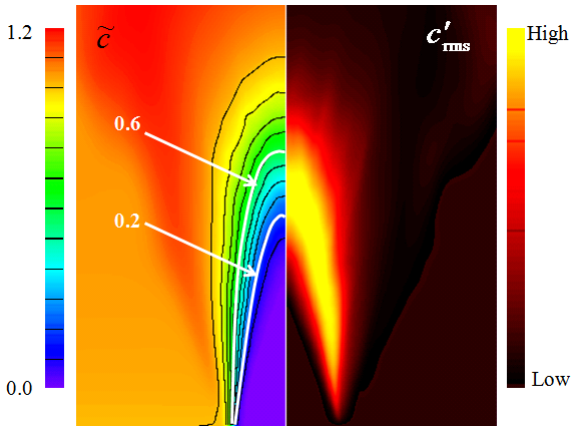

Figure 5. Distributions of Favre average ($\tilde{c}$) and r.m.s. (c''_{rms}) of reaction progress variable for HJ60.

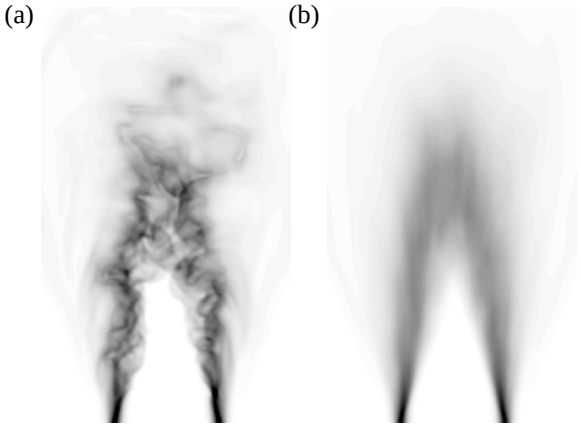

Figure 6. Instantaneous distribution of temperature gradient integrated in z direction (a), and its time-averaged distribution (b) for HJ60.

fine-scale eddies is proportional to square root of second invariant of velocity gradient tensor. The thick axes show the strong swirling motion in this visualization manner. As for the freely-propagating flame, the number of fine-scale eddies decreases through flame front significantly. Eddies become weak near flame front, and stretched in the streamwise direction. As for turbulent jet premixed flame, a lot of axes which are perpendicular to streamwise direction can be found behind main flame body, as shown by orange ellipses in Fig. 4(b) for instance. These eddies near flame front are related to formation of unburnt mixture islands. Near shear layer, thin and long axes which are parallel to streamwise direction are generated. These axes correspond to eddies which are induced by velocity difference due to strong dilatation.

CHARACTERISTICS OF TURBULENT PLANE JET PREMIXED FLAME

In this section, HJ60 is focused on, since characteristic flame structure, the unburnt mixture island, is generated. The analysis results of HJ97 will be presented in another opportunity. Figure 5 shows distributions of Favre average ($\tilde{c}$) and r.m.s. (c''_{rms}) of reaction progress variable ($c = (T - T_u)/(T_b - T_u)$). Here, T_u and T_b are temperature of unburnt mixture at inlet and that of burnt gas. c''_{rms} spreads toward downstream and shows high values in $\tilde{c} = 0.2 \sim 0.6$, which means that flame fronts fluctuates significantly in the top of flame. Figure 6(a) and (b) shows the instantaneous distribution of temperature gradient integrated in z direction and its time-averaged distribution. Assuming that pressure change through flame is negligible, temperature gradient corresponds to density gradient, and hence Fig. 6 shows pseudo schlieren photograph of flame. The region of high time-averaged temperature gradient is similar to that of high c''_{rms} except for near inlet. Gray region represents the region with large flame fluctuation and becomes wider in downstream region. In the DNS of premixed flame propagating in homogeneous isotropic turbulence, wide flame brush is formed by wrinkling, multi-layers and multi-folding of flame front (Shim et al., 2011). However, even though the combustion condition of the present DNS is classified into the corrugated flamelets regime, wide flame brush is generated not only due to flame wrinkling but also to frequently formation of unburnt mixture islands in burnt region.

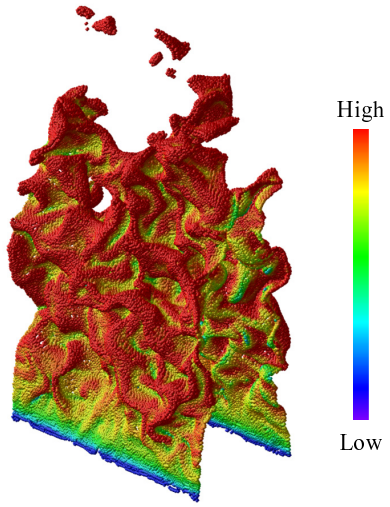

Figure 7. Distribution of local heat release rate on flame front for HJ60.

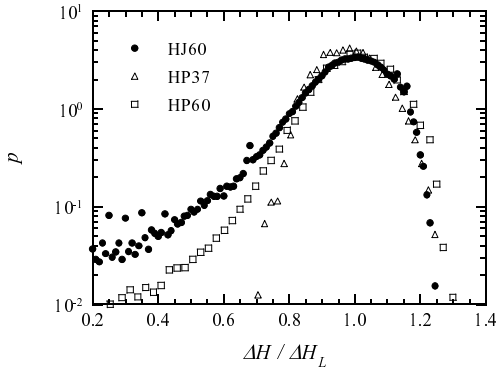

Figure 8. Probability density functions of the maximum heat release rate in local flame elements for HJ60, HP37 and HP60.

Figure 7 shows distribution of local heat release rate on flame front. Flame front is defined by the position where temperature gradient is the maximum locally. Flame is ignited near inlet by surrounding burnt gas and relatively flat flame, which shows low heat release rate, is generated. Flame front is distorted by strong turbulence in unburnt mixture. In the downstream region, complicated flame structure is generated, and heat release rate increases. Heat release rate at flame front convex toward burnt side tends to be high, and that at flame front convex toward unburnt side tends to be low. This trend is similar to that of turbulent premixed flame freely propagating in homogeneous isotropic turbulence (Shim et al., 2011).

Figure 8 shows pdf of the maximum heat release rate in local flame elements. For comparison, the results in turbulent premixed flame freely propagating in homogeneous isotropic turbulence HP37 and HP60 are also plotted. Local heat release rate is normalized by the maximum value of heat release rate in laminar premixed flame (ΔH_L). The pdf of local heat release rate has peak at around ΔH_L. Variance of pdf for HP60 is larger than that for HP37 due to higher Reynolds number. Variance of pdf for HJ60 is further large, since jet flame has a lot of flame elements which shows low heat release rate due to ignition near the nozzle. Flame elements

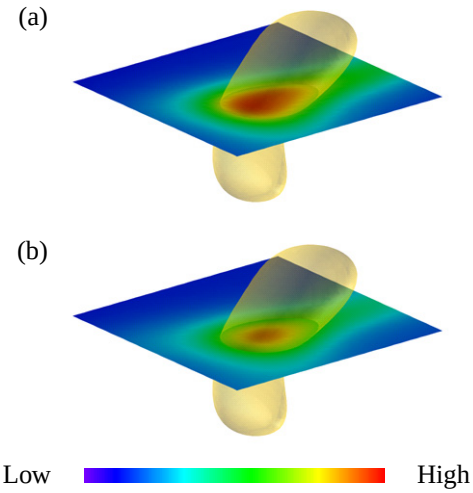

Figure 9. Distributions of reaction rate of R6 (a) and mass fraction of HO_2 (b) near isolated unburnt mixture island shown in Fig. 2(a).

with high heat release rate increases with increase of turbulent intensity for HP37 and HP60. The coherent fine-scale eddy which is parallel to flame front transports unburnt mixture into the flame front by a strong swirling motion and generates flame front with high heat release rate (Tanahashi et al., 2000). Although turbulent intensity of HJ60 is about two-thirds for HP37 and one-third for HP60, turbulent plane jet premixed flame HJ60 has flame elements with high heat release rate as much as HP37 around $\Delta H_L/\Delta H_L = 1.20$ and HP60 around $\Delta H_L/\Delta H_L = 1.15$. This can be explained by the characteristic structure of turbulent plane jet premixed flame; the unburnt mixture island.

Figure 9(a) and (b) shows distributions of reaction rate of R6 ($H+O_2$ (+M) $\Leftrightarrow$ HO_2 (+M)) and mass fraction of HO_2 near isolated unburnt mixture island. The temperature of the unburnt mixture island increases due to the heat conduction from surrounding burnt gas. The temperature rise enhances rate of chemical reaction R6 and HO_2 concentration as shown in Fig. 9 (Tanahashi et al., 2002; Nada et al., 2004). HO_2 is consumed to produce OH radical rapidly. In turbulent jet premixed flame, frequent creations of unburnt mixture island by fine-scale eddies in turbulence increases turbulent burning velocity.

CONCLUSIONS

Three-dimensional DNS of hydrogen–air turbulent plane jet premixed flame has been conducted to investigate shear effects on flame and eddy structures. In turbulent plane jet premixed flame, eddy structures which have large-scale in space and streamwise rotating axis are produced along the outer edge of OH layer in burnt gas by velocity difference due to strong dilatation. For the case with high inlet velocity, Kelvin-Helmholtz rollers are induced by the large velocity difference between unburnt and burnt gases, and the rib structures are formed in the braid region. Although combustion condition of the present DNS is classified into corrugated flamelets regime, unburnt mixture islands frequently appear

behind the main flame. Identification of axes of coherent fine-scale eddies revealed that a lot of eddies which are perpendicular to the streamwise direction exist behind main flame and are closely related to the creation of unburnt mixture islands. The unburnt mixtures are consumed rapidly by heating from surrounding burnt gas, which results in increase burning velocity of jet flames.

ACKNOWLEDGMENTS

This work is partially supported by the Cabinet Office, Government of Japan through its " Funding Program for Next Generation World-Leading Researchers".

REFERENCES

Baum, M., Poinsot, T., and Thevenin, D., 1994, "Accurate Boundary Conditions for Multicomponent Reactive Flows", Journal of Computational Physics, Vol. 106, pp. 247–261.

Candel, S. M., and Poinsot, T. J., 1990, "Flame Stretch and the Balance Equation for the Flame Area", Combustion Science and Technology, Vol. 70, pp. 1–15.

Clavin, P., 1985, "Dynamic Behavior of Premixed Flame Fronts in Laminar and Turbulent Flows", Progress in Energy and Combustion Science, Vol. 11, pp. 1–59.

Driscoll, J. F., 2008, "Turbulent Premixed Combustion: Flamelet Structure and its Effect on Turbulent Burning Velocity", Progress in Energy and Combustion Science, Vol. 34, pp. 91–134.

Hawkes, E. R., Sankaran, R., Chen, J. H., Kaiser, S. A., and Frank, J. H., 2009, "An Analysis of Lower-Dimensional Approximations to the Scalar Dissipation Rate Using Direct Numerical Simulations of Plane Jet Flames", Proceedings of the Combustion Institute, Vol. 32, pp. 1455–1463.

Kee, R. J., Dixon-Lewis, G., Warnatz, J., Coltrin, M. E., and Miller, J. A., 1986, "A Fortran Computer Code Package for the Evaluation of Gas-Phase, Multicomponent Transport Properties", Sandia Report, No. SAND86-8246, Sandia National Laboratories.

Kee, R. J., Rupley, F. M., and Miller, J. A., 1989, "CHEMKIN-II: A Fortran Chemical Kinetics Package for the Analysis of Gas Phase Chemical Kinetics", Sandia Report No. SAND89-8009B, Sandia National Laboratories.

Law, C. K., and Sung, C. J., 2000, "Structure, Aerodynamics, and Geometry of Premixed Flamelets", Progress in Energy and Combustion Science, Vol. 26, pp. 459–505.

Lele, S. K., 1992, "Compact Finite Difference Schemes with Spectral-Like Resolution", Journal of Computational Physics, Vol. 103, pp. 16–42.

Miller, J. A., and Bowman, C. T., 1989, "Mechanism and Modeling of Nitrogen Chemistry in Combustion", Progress in Energy and Combustion Science, Vol. 15, pp. 287–338.

Nada, Y., Tanahashi, M., and Miyauchi, T., 2004, "Effect of Turbulence Characteristics on Local Flame Structure of H_2–Air Premixed Flames", Journal of Turbulence, Vol. 5, ARTN016.

Peter, N. B., George, D. B., and Alan, C. H., 1989, "VODE, a Variable-Coefficient ODE Solver", SIAM Journal of Scientific and Statistical Computation, Vol. 10, pp. 1038–1051.

Peters, N., 2000, "Turbulent Combustion", London: Cambridge Press.

Poinsot, T. J, Echekki, T., and Mungal, M. G., 1992a, "A Study of the Laminar Flame Tip and Implications for Premixed Turbulent Combustion", Combustion Science and Technology, Vol. 81, pp. 45–73.

Poinsot, T. J. and Lele, S. K., 1992b, "Boundary conditions for direct simulations of compressible viscous flows", Journal of Computational Physics, Vol. 101, pp. 104–129.

Pope, S. B., 1988, "The Evolution of Surface in Turbulence", International Journal of Engineering Science, Vol. 26, pp. 445–469.

Shim, Y.-S., Tanaka, S., Tanahashi, M., and Miyauchi, T., 2011, "Local Structure and Fractal Characteristics of H_2–Air Turbulent Premixed Flame", Proceedings of the Combustion Institute, Vol. 33, pp. 1455–1462.

Sinibaldi, J. O., Driscoll, J. F., Muller, C. J., Donbar, J. M., and Carter, C. D., 2003, "Propagation Speeds and Stretch Rates Measured along Wrinkled Flames to Assess the Theory of Flame Stretch", Combustion and Flame, Vol. 133, pp. 323–334.

Smooke, M. D., and Giovangigli, V., 1991, "Formulation of the Premixed and Nonpremixed Test Problems, Reduced Kinetic Mechanisms and Asymptotic Approximations for Methane–Air Flames", Springer-Verlag, pp. 1–28.

Steinberg, A. M., and Driscoll, J. F., 2010, "Stretch-Rate Relationships for Turbulent Premixed Combustion LES Subgrid Models Measured Using Temporally Resolved Diagnostics", Combustion and Flame, Vol. 157, pp. 1422–1435.

Tanahashi, M., Miyauchi, T., and Ikeda, J., 1999, Simulation and Identification of Organized Structures in Flow, pp. 131–140.

Tanahashi, M., Fujimura, M., and Miyauchi, T., 2000, "Coherent Fine-Scale Eddies in Turbulent Premixed Flames", Proceedings of the Combustion Institute, Vol. 28, pp. 529–535.

Tanahashi, M., Iwase, S., and Miyauchi, T., 2001, "Appearance and Alignment with Strain Rate of Coherent Fine Scale Eddies in Turbulent Mixing Layer", Journal of Turbulence, Vol. 2, ARTN006.

Tanahashi, M., Nada, Y., Ito, Y., and Miyauchi, T., 2002, "Local Flame Structure in the Well-Stirred Reactor Regime", Proceedings of the Combustion Institute, Vol. 29, pp. 2041–2049.

Tanahashi, M., Kang, S.-J., Miyamoto, T., Shiokawa, S., and Miyauchi, T., 2004, "Scaling Law of Fine Scale Eddies in Turbulent Channel Flows up to $Re\tau = 800$", International Journal of Heat and Fluid Flow, Vol. 25, pp. 331–340.

Wang, Y., Tanahashi, M., and Miyauchi, T., 2007, "Coherent Fine Scale Eddies in Turbulence Transition of Spatially-Developing Mixing Layer", International Journal of Heat and Fluid Flow, Vol. 28, pp. 1280–1290.

Williams, F. A., 2000, "Progress in Knowledge of Flamelet Structure and Extinction", Progress in Energy and Combustion Science, Vol. 26, pp. 657–682.

Yamawaki, K., Shim, Y.-S., Fukushima, N., Shimura, M., Tanahashi, M., and Miyauchi, T., 2010, "Numerical Study on Dynamics of Local Flame Elements in Turbulent Jet Premixed Flames", IOP Conference Series: Material Science and Engineering, Vol. 10, 012032.